Inorganic Chemistry

Article

pubs.acs.org/IC

Synthesis of V/Fe/S Clusters Using Vanadium(III) Thiolate Complexes Bearing a Phenoxide-Based Tridentate Ligand

Nobuhiro Taniyama, Yasuhiro Ohki, and Kazuyuki Tatsumi*

Department of Chemistry, Graduate School of Science and Research Center for Materials Science, Nagoya University, Furo-cho, Chikusa-ku, Nagoya 464-8602, Japan

Supporting Information

ABSTRACT: Vanadium(III) thiolate complexes carrying a phenoxide-based tridentate ligand were prepared from the reactions of $V(NMe_2)_4$ with the protonated forms of tridentate ligands (H_2(O,P,O) = bis(3,5-di-*tert*-butyl-2-hydroxyphenyl)-phenylphosphine or H_2(O,O,O) = bis(3,5-di-*tert*-butyl-2-hydroxyphenyl)phenyl-phosphineoxide) and thiols (HSR; R = mesityl (Mes), 2,4,6-^{i}Pr$_3$C$_6$H$_2$ (Tip)). The vanadium−thiolate complexes were subjected to the V/Fe/S cluster synthesis via treatment with an Fe(II) thiolate complex $[(TipS)Fe]_2(\mu$-SDmp$)_2$ (**4**, Dmp = 2,6-(mesityl)$_2$C$_6$H$_3$) and elemental sulfur in toluene, leading to the formation of two new V/Fe/S clusters. One is an edge-bridged double-cubane-type $[VFe_3S_4]$-$[VFe_3S_4]$ cluster $[$(O,P,O)VFe_3S_4(SDmp)$(HNMe_2)]_2$ (**5**) having face-capping tridentate (O,P,O) ligands on vanadium atoms. The other is a $[VFe_3S_4$-Fe] cluster $[(\mu$-O,O,O)VFe_3S_4(SDmp)(STip)Fe$(\mu$-SDmp)] (**6**), the core of which consists of a cubane-type $[VFe_3S_4]$ unit and an external iron atom. The external iron is bound to an SDmp ligand and two oxygen atoms of the tridentate (O,O,O) ligand. Cluster **6** is structurally relevant to the active site of nickel-dependent CO dehydrogenase, and their common structural features include a cubane-type unit with a heterometal, one more iron atom besides the cubane unit, and a bridging ligand between the external iron and the heterometal of the cubane unit.

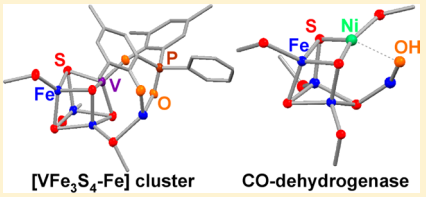

INTRODUCTION

Metal−sulfur clusters are abundant in living organisms, mediating electron transfer and chemical transformations.[1−3] While the majority of these clusters are iron−sulfur clusters, some clusters with two transition elements have been found in the active sites of metalloenzymes involved in small molecule activation. Representative examples include the FeMo-cofactor of nitrogenase, which catalyzes the reduction of N_2 into NH_3,[4] the FeV-cofactor of vanadium-dependent nitrogenase,[5] and the $[NiFe_4S_4]$ cluster active site of nickel-dependent CO dehydrogenase, which catalyzes the interconversion between CO and CO_2 (Chart 1).[3b,6] The complicated structures and the reducing activities of these clusters have been attracting interests, and hence, they have been important synthetic targets for inorganic chemists. Thus far, Holm and co-workers have synthesized a series of M/Fe/S (M = Mo, V) clusters topologically analogous to the nitrogenase P-cluster,[7] and they have also prepared $[NiFe_3S_4]$ cubane-type clusters mimicking the active site of CO dehydrogenase.[8] Coucouvanis et al. have reported some incomplete cubane-type $[MoFe_3S_3]$ clusters carrying a catecholate and a pyridine ligand on molybdenum, which can be seen as a fragment of the FeMo-cofactor.[9] Notably, for the assembly of these cluster cores, polar organic solvents (i.e., CH_3CN and CH_3OH) have been commonly used to dissolve the ionic reactants, such as tetrathio-molybdates, thiolates, and iron chlorides.

We have developed a synthetic method to prepare iron−sulfur clusters in toluene and have successfully synthesized a series of clusters mimicking the metalloclusters in nitrogenase[10] and high-potential iron−sulfur proteins.[11] As shown in Scheme 1, the reaction of an Fe(II) thiolate complex with elemental sulfur in toluene was found to give an $[Fe_8S_7]$ cluster $[Fe_4S_3$(SDmp)$]_2(\mu$-SDmp$)_2(\mu$-STip$)(\mu_6$-S) (**A**; Tip = 2,4,6-^{i}Pr$_3$C$_6$H$_2$, Dmp = 2,6-(mesityl)$_2$C$_6$H$_3$).[10b] In contrast to

Chart 1. Nitrogenase FeMo-Cofactor and the Active Site of Ni-Dependent CO Dehydrogenase. Cys = Cysteine, His = Histidine

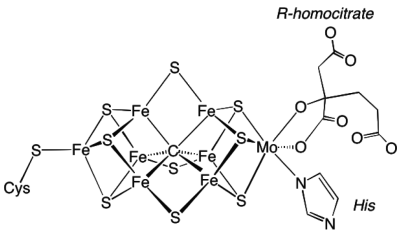

FeMo-cofactor

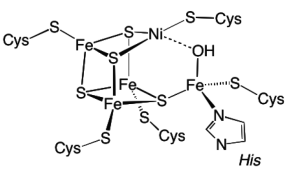

active site of Ni-dependent CO dehydrogenase

Received: December 13, 2013
Published: May 19, 2014

 © 2014 American Chemical Society dx.doi.org/10.1021/ic4030603 | Inorg. Chem. 2014, 53, 5438−5446

Scheme 1

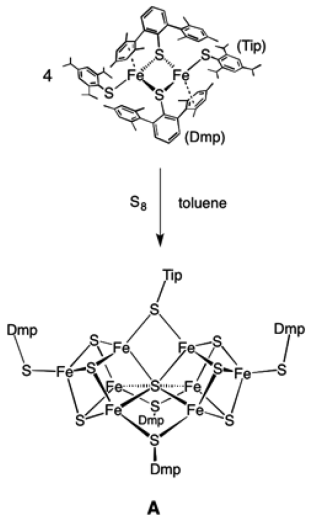

ordinary synthetic iron–sulfur clusters with four or less than four iron atoms, cluster **A** contains eight iron atoms and has an intriguing structural relevance to the FeMo-cofactor in that two $[M_4S_3]$ incomplete cuboidal units (M = metals) are connected by a central μ_6 atom and three bridging sulfur donors. The successful synthesis of FeMo-cofactor mimic **A** prompted us to expand the scope of this reaction for the synthesis of V/Fe/S clusters, by incorporating vanadium complexes into the reaction mixture. As our cluster synthesis is carried out in toluene, a series of new vanadium–thiolate precursors were prepared in this study from the reactions of $V(NMe_2)_4$ (**1**)[12] with tridentate ligands and thiols. Chart 2 shows the phenoxide-based

Chart 2. Tridentate Ligands Used in This Study

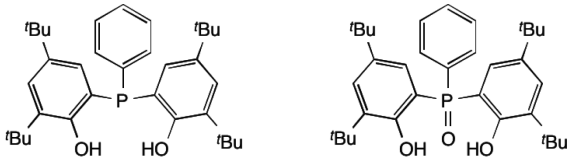

tridentate ligands, whose protonated forms are denoted as $H_2(O,P,O)$ and $H_2(O,O,O)$ in this paper ($H_2(O,P,O)$ = bis(3,5-di-*tert*-butyl-2-hydroxyphenyl)phenylphosphine, $H_2(O,O,O)$ = bis(3,5-di-*tert*-butyl-2-hydroxyphenyl)phenylphosphineoxide).[13] The (O,P,O) ligand has been demonstrated to coordinate to Ti, V, Ta, Co, and Rh as a facial tridentate ligand,[13,14] and the (O,O,O) ligand is available via oxidation of $H_2(O,P,O)$ with H_2O_2.[13] Herein, we report the reactions of new vanadium–thiolate complexes with an Fe(II) thiolate complex and elemental sulfur in toluene, leading to the formation of two new V/Fe/S clusters. One of the new clusters is an edge-bridged double-cubane-type $[VFe_3S_4]$-$[VFe_3S_4]$ cluster, and the other is a $[VFe_3S_4$-Fe] cluster that is structurally relevant to the active site of nickel-dependent CO dehydrogenase.

RESULTS AND DISCUSSION

Synthesis of V(III)–Thiolate Complexes Having a Tridentate Ligand. In this study, vanadium(IV) amide complex $V(NMe_2)_4$ (**1**) was used as the precursor to synthesize new vanadium–thiolate complexes. Complex **1** was treated with the protonated forms of tridentate ligands $H_2(O,P,O)$ or $H_2(O,O,O)$ and then with 2 equiv of thiols, resulting in the formation of the V(III)–thiolate complexes bearing a tridentate ligand and a dimethylamine ligand, $(O,P,O)V(SR)(HNMe_2)$ (**2a**, R = (mesityl) Mes; **2b**, R = 2,4,6-^{i}Pr$_3$C$_6$H$_2$ (Tip)) or $(O,O,O)V(SR)(HNMe_2)$ (**3a**, R = Mes; **3b**, R = Tip) (Scheme 2). The first step of the reaction sequence of Scheme 2 involves

Scheme 2

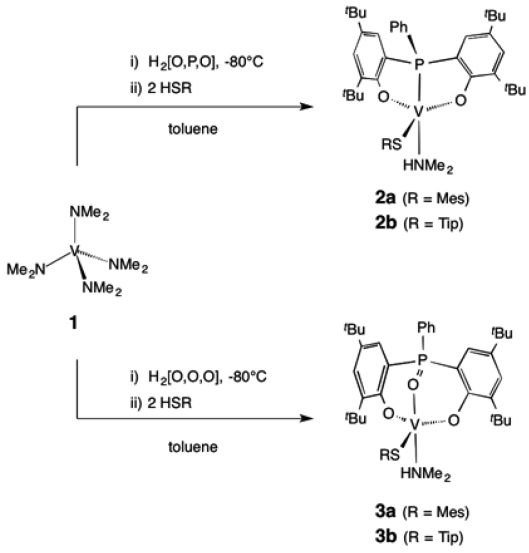

the replacement of two amide ligands with a tridentate ligand via proton transfer to generate a putative intermediary complex $(O,E,O)V(NMe_2)_2$ (E = O, P), in which amide ligands take up protons from thiols in the following step. These proton transfer reactions provide dimethylamine, which serves as a ligand in complexes **2a–2b** and **3a–3b**. Whereas the replacement of amide ligands in $(O,E,O)V(NMe_2)_2$ with thiolates is expected to give a V(IV) complex $(O,E,O)V(SR)_2$, the products in Scheme 2 are V(III) complexes with one thiolate ligand. Dissociation of an –SR group from the tentative intermediate $(O,E,O)V(SR)_2$ accounts for the reduction from V(IV) to V(III), while the possible byproduct RS-SR has not been detected.

The V(III) oxidation state of complexes **2a–2b** and **3a–3b** was supported by the EPR spectra and the magnetic susceptibility measurements. The room-temperature EPR spectra of complexes **2a–2b** (in THF) and **3a–3b** (in toluene) were silent, as the V(III) complexes with low symmetry are known to become EPR-silent at conventional frequencies and fields.[15] The silent EPR spectra are inconsistent with the EPR-active V(IV) state (d^1 configuration), which is expected to give an $S = 1/2$ signal. Temperature-dependent magnetic susceptibilities of complexes **2a–2b** and **3a–3b** were measured by the SQUID magnetometer (Supporting Information, Figure S2). The effective magnetic moments of these complexes are nearly constant in the range of 50–300 K, μ_{eff} = 2.76–2.94 μ_B (**2a**), 2.51–2.74 μ_B (**2b**), 2.54–2.55 μ_B (**3a**), and 2.46–2.65 μ_B (**3b**). In agreement with the V(III) state (d^2 configuration), these magnetic moments are similar to the spin-only value for the $S = 1$ state (2.83 μ_B). The cyclic voltammograms (CVs) for **2a–2b** and **3a–3b** were measured in THF at room

dx.doi.org/10.1021/ic4030603 | Inorg. Chem. 2014, 53, 5438–5446

temperature using [nBu$_4$N][PF$_6$] as an electrolyte, where some irreversible oxidation and reduction waves appeared (Figure S3, Supporting Information). The common features are the reduction waves at E_{pc} = −2.08 to −2.27 V, and the oxidation waves of the corresponding species after reducing V(III) complexes appearing at E_{pa} = −1.33 to −1.37 V. These reduction/oxidation waves are coupled, and therefore, the oxidation waves at −1.33 to −1.37 V were not found in the CVs measured in the range of 0 to −2.0 V. In the CVs of **2a**−**3b** scanning toward positive potentials up to 1.0 V, large irreversible oxidation waves were observed at E_{pa} = 0.18−0.35 V. These waves would be assigned as the oxidation from V(III) to V(IV), and one of the possibilities accounting for the irreversibility is the dissociation of an −SR group from vanadium as 1/2 RS-SR.

The molecular structures of complexes **2a**−**2b** and **3a**−**3b** were determined by X-ray crystallographic analysis, and perspective views of **2a** and **3a** are shown in Figure 1 (others shown in the Supporting Information). The vanadium center is five-coordinate in these V(III)−thiolate complexes, with a tridentate ligand occupying two equatorial and one axial position. The dimethylamine ligand is located at the axial position, while the thiolate ligand is on the equatorial plane. The atoms in axial positions are linearly aligned with vanadium (P−V−N 166.28(6)° for **2a** and O−V−N 178.06(6)° for **3a**). The sums of S−V−O and O−V−O angles in the equatorial plane are 359.76(17)° (**2a**) and 359.92(16)° (**3a**). The V−S bond distances of **2a** (2.2931(8) Å) and **3a** (2.3136(8) Å) are close to those in a trigonal-bipyramidal V(III) complex V(STip)$_3$(THF)$_2$ (2.308(1)−2.334(1) Å).[16] The V−N(amine) distances of 2.178(3) Å (**2a**) and 2.2008(19) Å (**3a**) are also analogous to those in V(III)−amine complexes (2.146(7)−2.290(2) Å).[17]

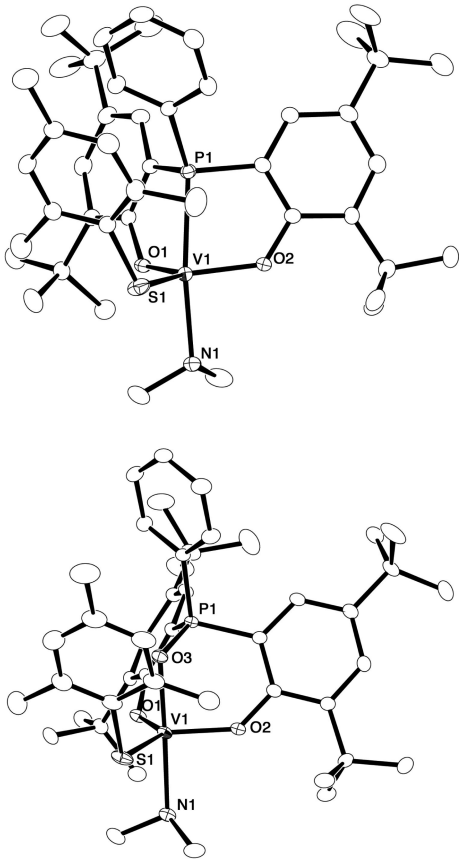

Figure 1. Molecular structures of **2a** and **3a** with thermal ellipsoids at the 30% probability level. Selected distances (Å) and angles (deg): **2a**: V1−S1 = 2.2931(8), V1−P1 = 2.4624(7), V1−O1 = 1.8911(17), V1−O2 = 1.8976(16), V1−N1 = 2.178(3); S1−V1−P1 = 102.44(3), S1−V1−O1 = 119.51(6), S1−V1−O2 = 125.12(6), S1−V1−N1 = 91.28(6), P1−V1−O1 = 81.09(6), P1−V1−O2 = 80.78(5), P1−V1−N1 = 166.28(6), O1−V1−O2 = 115.13(7), O1−V1−N1 = 91.94(8), O2−V1−N1 = 91.67(8). **3a**: V1−S1 = 2.3136(8), V1−O1 = 1.9026(13), V1−O2 = 1.8921(16), V1−O3 = 2.0332(15), V1−N1 = 2.2008(19); S1−V1−O1 = 130.65(5), S1−V1−O2 = 122.67(5), S1−V1−O3 = 91.53(5), S1−V1−N1 = 88.40(5), O1−V1−O2 = 106.60(6), O1−V1−O3 = 89.57(6), O1−V1−N1 = 89.01(6), O2−V1−O3 = 91.66(6), O2−V1−N1 = 90.01(7), O3−V1−N1 = 178.06(7).

Reactions of V(III) Thiolate Complexes with an Fe(II) Thiolate Complex and Elemental Sulfur. *(O,P,O)V Complex.* The V(III)−thiolate complexes were incorporated into a mixture of **4** and S_8 for the synthesis of V/Fe/S clusters. Considering the rapid reaction of **2a** with elemental sulfur, we mixed the reactants in the order of **4**, elemental sulfur, and **2a** in toluene. From the reaction of **4** with S_8 and **2a** in the ratio of V:Fe:S = 1:3:4, an edge-bridged double-cubane-type [VFe_3S_4]-[VFe_3S_4] cluster [(O,P,O)VFe_3S_4(SDmp)(HNMe$_2$)]$_2$ (**5**) was obtained in 22% yield as black needles (Scheme 3). While some edge-bridged double-cubane-type [VFe_3S_4]-[VFe_3S_4] clusters have been reported,[18] the $[V_2Fe_6S_8]^{6+}$ state of **5** is much higher than the known $[V_2Fe_6S_8]^{2+}$ clusters. The unique oxidation state of **5** shows the accessibility of a wide range of oxidation states in the edge-bridged double-cubane clusters. The effective magnetic moment of **5** in the solid state gradually decreases upon lowering the temperature, from 3.10 μ_B at 300 K to 0.89 μ_B at 2 K (Figure S5, Supporting Information), and the moment at 2 K is lower than the spin-only value for the S = 1/2 state (1.73 μ_B). On the other hand, the EPR spectrum of **5** in frozen toluene at 8 K[19] exhibited an S = 1/2 signal at g = 2.01 with multiple lines due to the nuclear spin of vanadium (Figure S6, Supporting Information). This result is inconsistent with the even number of electrons present in the centrosymmetric cluster **5**, as the odd number of electrons are required for the appearance of the S = 1/2 signal. We speculate two possible reasons: (i) partial contamination of the 1e-oxidized species with one missing hydrogen atom in one of the HNMe$_2$ ligands or the 1e-reduced species with an additional hydrogen atom on one of the oxygen/sulfur atoms in the same crystals, and (ii) partial decomposition of **5** in solution. The reason remains unclear, while the magnetic moment of 0.89 μ_B at 2 K for crystal samples is in between the S = 0 and 1/2 states. In the cyclic voltammogram of **5** in THF, an irreversible reduction wave was observed at −1.06 V vs Ag/AgNO$_3$ (Figure S7, Supporting Information). The possible reasons for the irreversibility of the reduction wave include the dissociation of HNMe$_2$ from iron and the splitting of the [VFe_3S_4]-[VFe_3S_4] cluster into two [VFe_3S_4] clusters upon reduction. Therefore, the measurement was also carried out in the presence of dimethylamine (2−4 equiv), but the reduction wave remained irreversible and one more reduction wave appeared at E_{pc} = −1.14 V. The second wave may come from the monomeric [VFe_3S_4] species, which is possibly generated via the splitting of the [VFe_3S_4]-[VFe_3S_4] cluster and the coordination of HNMe$_2$ to iron. The addition of a large excess (>20 equiv) of dimethylamine resulted in the disappearance of the reduction wave, indicating the degradation of the cluster.

dx.doi.org/10.1021/ic4030603 | Inorg. Chem. 2014, 53, 5438−5446

Scheme 3

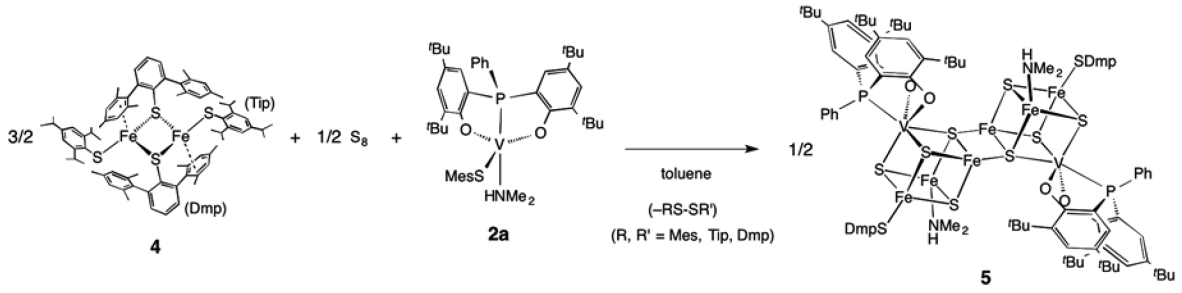

The molecular structure of **5** was determined by crystallographic analysis, as shown in Figure 2, whereas the insufficient quality of thin needle crystals enables limited discussion on the structure. Cluster **5** consists of two cubane-type units, each consisting of one vanadium carrying a face-capping (O,P,O) ligand, three irons, and four sulfurs. The two $[VFe_3S_4]$ units are connected through one of the Fe–S edges of cubes, defining an Fe_2S_2 rhomb in the middle. In analogy to the precedent edge-bridged double-cubane-type $[VFe_3S_4]$-$[VFe_3S_4]$ clusters,[18] the intracubane Fe–S distance within the rhomb (Fe2–S4, 2.357(5) Å) is longer than the intercubane Fe–S distance (Fe2–S4′, 2.280(5) Å). In contrast to the precedent $[VFe_3S_4]$-$[VFe_3S_4]$ clusters with peripheral vanadium atoms, the (O,P,O) V groups in **5** are located next to the central Fe_2S_2 rhomb. Another notable difference between the $[V_2Fe_6S_8]^{6+}$ cluster **5** and the precedent $[V_2Fe_6S_8]^{2+}$ clusters is the oxidation state, and the oxidation states of metals in **5** would be assigned as $V(III)_2Fe(II)_2Fe(III)_4$ or $V(IV)_2Fe(II)_4Fe(III)_2$. Although the higher oxidation state of **5** is expected to lead to the shorter V–S and V–Fe distances due to the smaller radius of metals, the V–S distances ranging from 2.385(5) to 2.436(4) Å are longer than those of the known $[VFe_3S_4]$-$[VFe_3S_4]$ clusters (2.35(2)–2.372(2) Å), and the V–Fe distances of **5** (2.789(4)–3.165(6) Å) are also longer than those of precedent clusters (2.702(2)–2.831(2) Å). Among the V–Fe distances of **5**, V–Fe1 (3.165(6) Å) is particularly long possibly because the phenyl group of the (O,P,O) ligand is orienting toward the thiolate ligand on Fe1, causing a steric congestion.

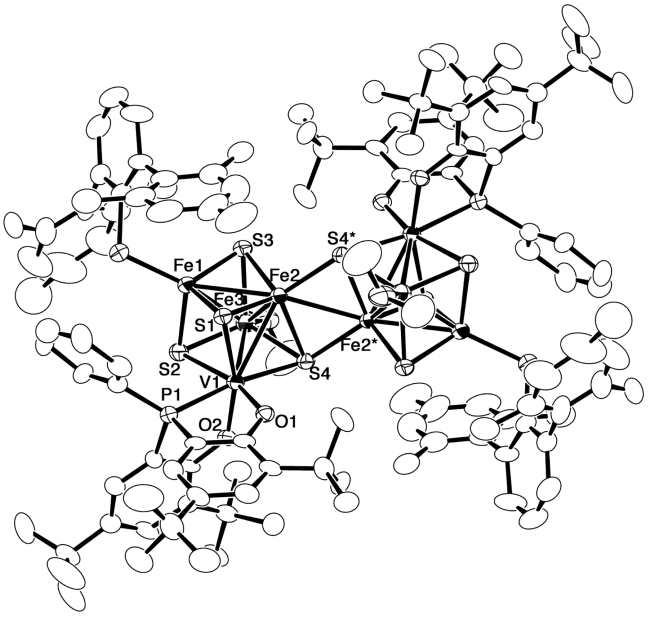

Figure 2. Molecular structure of **5** with thermal ellipsoids at the 30% probability level. Selected distances (Å) and angles (deg): V1–S1 = 2.385(5), V1–S2 = 2.436(4), V1–S4 = 2.420(5), V–O1 = 1.925(7), V1–O2 = 1.891(10), V1–P1 = 2.388(5), V1–Fe2 = 2.789(4), V1–Fe3 = 2.837(4), Fe1–Fe2 = 2.703(3), Fe1–Fe3 = 2.730(4), Fe2–Fe3 = 2.561(5), Fe2–Fe2′ = 2.716(4), Fe1–S1 = 2.293(4), Fe1–S2 = 2.276(5), Fe1–S3 = 2.210(5), Fe1–S5 = 2.194(4), Fe2–S1 = 2.218(5), Fe2–S3 = 2.281(5), Fe2–S4 = 2.357(5), Fe2–S4′ = 2.280(5), Fe3–S2 = 2.212(5), Fe3–S3 = 2.277(5), Fe3–S4 = 2.312(4); Fe2–S4–Fe2′ = 71.69(13), S4–Fe2–S4′ = 108.31(13).

(O,O,O)V Complex. Encouraged by the preparation of a double-cubane-type cluster **5**, the V/Fe/S cluster synthesis was also examined with the (O,O,O)V–thiolate complex **3b**. When complex **3b** was mixed with an iron–thiolate complex **4** and then with elemental sulfur in the ratio of V:Fe:S = 1:4:4, black crystals of a cubane-type cluster carrying an external iron atom, $[(\mu\text{-O,O,O})VFe_3S_4(SDmp)(STip)Fe(\mu\text{-SDmp})]$ (**6**), was obtained in 10% yield (Scheme 4). An analogous reaction using **3a** (bearing an –SMes ligand) also gave rise to the same cluster **6** in 8% yield, indicating that the thiolate ligands in the vanadium precursors readily dissociate upon treatment with elemental sulfur. The magnetic moment of **6** was observed to be similar in the range of 50–300 K, μ_{eff} = 4.38–4.80 μ_B (Figure S8, Supporting Information), which is close to the spin-

Scheme 4

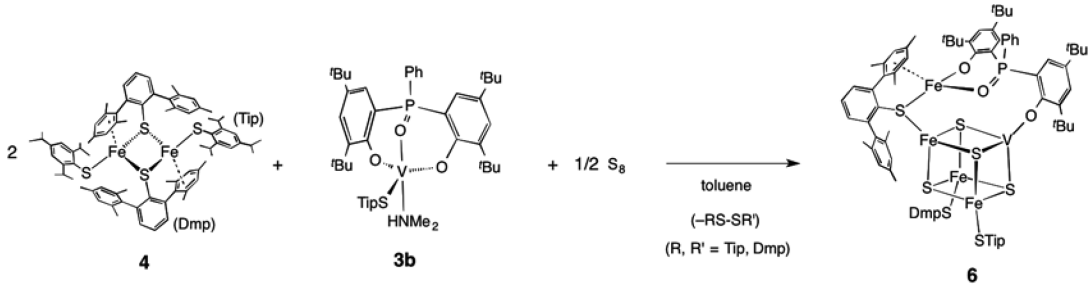

dx.doi.org/10.1021/ic4030603 | Inorg. Chem. 2014, 53, 5438–5446

only value for the $S = 2$ state (4.90 μ_B). There was no significant signal in the EPR spectrum of **6** in frozen toluene at 4−15 K,[19] while a few $[Fe(SR)_4]^{2-}$ compounds in the $S = 2$ system are known to exhibit EPR signals at around $g = 10$.[20] The cyclic voltammogram of **6** in THF was almost featureless, exhibiting very weak waves at $E_{pc} = -0.84$ V and $E_{pa} = -0.73$ and −0.45 V (Figure S9, Supporting Information). This may be due to the degradation of **6** in THF in the presence of electrolyte $[n\mathrm{Bu_4N}][PF_6]$. The external iron atom in **6** supported by the flexible (O,O,O) ligand and the bridging SDmp ligand may be released in an electrolyte solution of THF, and the four-coordinate vanadium would accommodate THF or fluoride ions from a PF_6 anion.

The molecular structure of $[VFe_3S_4\text{-}Fe]$ cluster **6** was determined by X-ray crystallographic analysis, and an ORTEP drawing is shown in Figure 3. Cluster **6** consists of a cubane-type $[VFe_3S_4]$ unit and an external iron atom (Fe4), which is linked to the cubane unit through a thiolate sulfur and two oxygen atoms of the (O,O,O) ligand. Although the external iron (Fe4) looks three-coordinate, there is a weak interaction between Fe4 and one of the mesityl rings of SDmp, completing the distorted tetrahedral geometry. The shortest Fe4−C42 contact of 2.480(4) Å is within the range of Fe−C(arene) interaction found for the Fe−SDmp complexes (2.389(2)−2.599(2) Å).[10b,e,21] The Fe4−S5 distance (2.3327(12) Å) is also comparable to those of Fe(II) complexes having μ-SDmp ligands,[10b,e,21] indicating the Fe(II) state for Fe4. The external Fe4 atom reveals no direct metal−metal interaction, and the shortest intermetallic distance is 3.6866(9) Å (Fe4−Fe1). Interestingly, the vanadium atom of **6** is four-coordinate, with three sulfido ligands and a phenoxide oxygen of the tridentate (O,O,O) ligand. This is in contrast to the precedent V/Fe/S clusters in which vanadium atoms are five- or six-coordinate.[18,22] Thus, the vanadium in **6** is more electron-deficient, resulting in the relatively short V−(μ_3-S) (2.2112(13)−2.2466(12) Å) and V−Fe (2.6422(9)−2.6873(10) Å) distances compared to those reported for the $[VFe_3S_4]$ and $[VFe_3S_4]$-$[VFe_3S_4]$ clusters (V−S, 2.303(1)−2.387(2) Å; V−Fe, 2.691(2)−2.8363(6) Å).[18,22] On the other hand, the Fe−Fe (2.6896(8)−2.7409(7) Å) and Fe−(μ_3-S) (2.2447(11)−2.2843(11) Å) distances in the $[VFe_3S_4]$ core of **6** are comparable to those reported for the $[VFe_3S_4]$ clusters (Fe−Fe, 2.569(2)−2.757(2) Å; Fe−(μ_3-S), 2.205(2)−2.326(2) Å).[22] The cubic core is rigid, and thus, distances and angles within the cubic core do not vary significantly by the oxidation state of metals. Further, metal−metal interactions lead to charge delocalization, hampering the assignments to specific oxidation states of metals. Nevertheless, the cubane unit of **6** is in the $[VFe_3S_4]^{3+}$ state, for which a tentative assignment of V(III)-Fe(II)$Fe(III)_2$ would be applied.

It is notable that the $[VFe_3S_4\text{-}Fe]$ core of cluster **6** has structural relevance to the $[NiFe_3S_4\text{-}Fe]$ cluster active site of nickel-dependent CO dehydrogenase. As shown in Figure 4, their common structural features include a cubane-type $[MFe_3S_4]$ core with a heterometal (M = V or Ni), one more iron atom besides the cubane core, and a bridging ligand between the external iron and the heterometal. The structure of **6** also reveals the flexibility of the tridentate (O,O,O) ligand, which appears to be important to accommodate the external iron atom. Cluster **6** incorporates vanadium as a heterometal; however, synthesis of nickel precursors bearing a flexible (O,O,O) ligand and their reactions with iron−thiolate complexes and elemental sulfur in toluene may provide $[NiFe_3S_4\text{-}Fe]$ clusters modeling the active site of CO dehydrogenase.

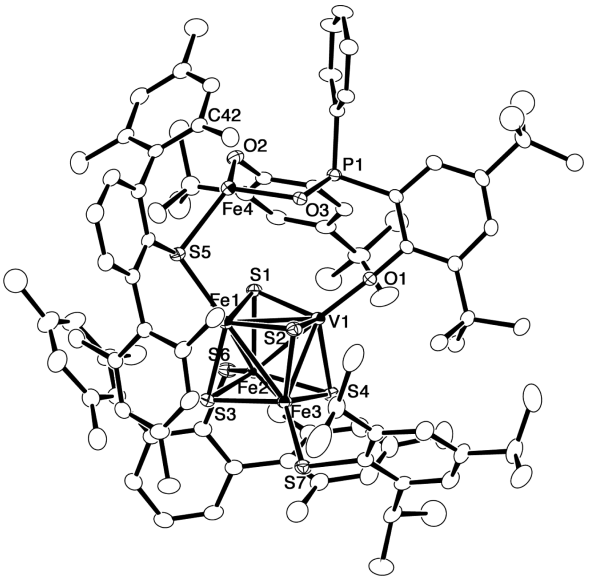

Figure 3. Molecular structure of **6** with thermal ellipsoids at the 30% probability level. Selected distances (Å) and angles (deg): V1−S1 = 2.2112(13), V1−S2 = 2.2384(12), V1−S4 = 2.2466(12), V−O1 = 1.786(3), V1−Fe1 = 2.6422(9), V1−Fe2 = 2.6873(10), V1−Fe3 = 2.6581(9), Fe1−Fe2 = 2.7409(7), Fe1−Fe3 = 2.6896(8), Fe2−Fe3 = 2.7330(8), Fe1−S1 = 2.2843(11), Fe1−S2 = 2.2486(13), Fe1−S3 = 2.2525(11), Fe1−S5 = 2.3118(11), Fe2−S1 = 2.2447(11), Fe2−S3 = 2.2577(11), Fe2−S4 = 2.2710(12), Fe2−S6 = 2.2243(13), Fe3−S2 = 2.2686(11), Fe3−S3 = 2.2510(13), Fe3−S4 = 2.2674(10), Fe3−S7 = 2.2232(13), Fe4−S5 = 2.3327(12), Fe4−O2 = 1.911(3), Fe4−O3 = 2.001(3), Fe4−C42 = 2.480(4); S1−V1−S2 = 107.09(5), S1−V1−S4 = 104.80(5), S1−V1−O1 = 113.10(10), S2−V1−S4 = 106.11(5), S2−V1−O1 = 110.53(10), S4−V1−O1 = 114.65(9), S1−Fe1−S2 = 104.29(4), S1−Fe1−S3 = 102.79(4), S1−Fe1−S5 = 88.43(4), S2−Fe1−S3 = 105.05(4), S2−Fe1−S5 = 118.49(5), S3−Fe1−S5 = 130.73(5), S1−Fe2−S3 = 103.89(4), S1−Fe2−S4 = 102.91(4), S1−Fe2−S6 = 96.32(5), S3−Fe2−S4 = 103.51(4), S3−Fe2−S6 = 122.25(5), S4−Fe2−S6 = 123.80(5), S2−Fe3−S3 = 104.44(5), S2−Fe3−S4 = 104.41(4), S2−Fe3−S7 = 114.23(5), S3−Fe3−S4 = 103.84(5), S3−Fe3−S7 = 114.69(5), S4−Fe3−S7 = 114.01(5), S5−Fe4−O2 = 125.53(10), S5−Fe4−O3 = 115.83(8), O2−Fe4−O3 = 96.62(12).

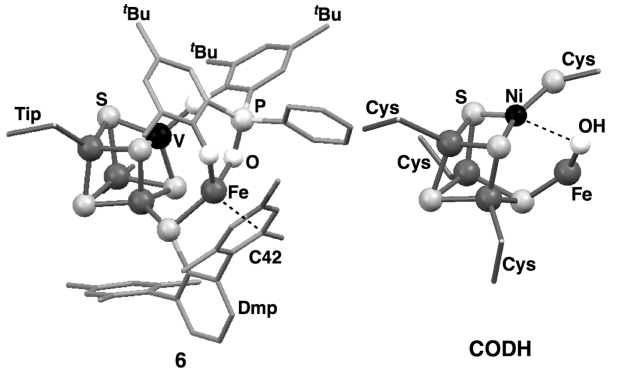

Figure 4. Structures of **6** and the active site of Ni-dependent CO dehydrogenase (CODH), emphasizing their structural relevance. Protein structural data is taken from PDB entry 3B51.[6b]

dx.doi.org/10.1021/ic4030603 | Inorg. Chem. 2014, 53, 5438−5446

CONCLUDING REMARKS

In this study, we have developed a new synthetic route to V/Fe/S clusters in toluene. A series of precursor vanadium(III) thiolate complexes **2a**−**2b** and **3a**−**3b** bearing a phenoxide-based tridentate ligand were synthesized from the reactions of vanadium(IV) amide complex **1** with H_2(O,P,O) or H_2-(O,O,O) and thiols. These vanadium(III) complexes were found to react with $[(TipS)Fe]_2(\mu\text{-SDmp})_2$ and elemental sulfur, producing two new V/Fe/S clusters **5** and **6**. Cluster **5** is an edge-bridged double-cubane-type $[VFe_3S_4]$-$[VFe_3S_4]$ cluster, and the position of (O,P,O)V units in **5** next to the central Fe_2S_2 rhomb is different from the known $[VFe_3S_4]$-$[VFe_3S_4]$ clusters in which vanadium atoms occupy the peripheral positions. Cluster **6** consists of a cubane-type $[VFe_3S_4]$ core and an external iron atom. Two oxygen atoms of the (O,O,O) ligand in **6** coordinate the external iron, leaving one phenoxide oxygen terminally bound to vanadium. One of the thiolate ligands is also bound to the external iron with its sulfur atom and an aromatic ring. The synthetic protocol demonstrated in this study would be applicable to the synthesis of Mo/Fe/S and Ni/Fe/S clusters in toluene, providing potential routes to structural mimics of the nitrogenase FeMo-cofactor and the active site of Ni-dependent CO dehydrogenase. In this regard, the successful preparation of **6** is particularly encouraging, as this cluster has structural relevance to the active site of CO dehydrogenase.

EXPERIMENTAL SECTION

General Procedures. All reactions were carried out using standard Schlenk techniques and a glovebox under a nitrogen atmosphere. Acetonitrile, diethyl ether, hexane, pentane, tetrahydrofuran, and toluene were purified by the method of Grubbs et al.,[23] where the solvents were passed over columns of activated alumina and a supported copper catalyst supplied by Hansen & Co. Ltd. The ^{1}H and $^{31}P\{^1H\}$ NMR spectra were recorded on a JEOL ECA-600. The proton signals were referenced to the residual signals of deuterated solvents. The $^{31}P\{^1H\}$ NMR chemical shifts are relative to the external reference of 85% H_3PO_4. The ^{31}P NMR of complexes **2a**−**2b** and **3a**−**3b** were measured in C_6D_6, but paramagnetism of these complexes led us to observe no assignable ^{31}P signals. In other words, detection sensitivity of the ^{31}P NMR is not good enough to clearly show the broadened paramagnetic signals. UV−vis spectra were measured on a JASCO V560 spectrometer. Elemental analyses were performed on a LECO CHNS-932 microanalyzer, where the crystalline samples were sealed into silver capsules in a glovebox. Cyclic voltammograms (CVs) were recorded in THF at room temperature using glassy carbon as the working electrode with 0.2 M $[^nBu_4N][PF_6]$ as the supporting electrolyte. The potentials were referenced to $Ag/AgNO_3$. The solid-state magnetic susceptibility was measured using a Quantum Design MPMS-XL SQUID-type magnetometer, and the samples were sealed in quartz tubes. The EPR spectrum was recorded on a Bruker EMX-plus spectrometer at X-band frequencies. X-ray diffraction data were collected on a Rigaku AFC8 or RA-Micro7 equipped with a CCD area detector using graphite monochromated Mo Kα radiation. $V(NMe_2)_4$ (**1**),[12a] $[(TipS)Fe]_2(\mu\text{-SDmp})_2$ (**4**),[10b] HSMes,[24] HSTip,[25] and bis(3,5-di-*tert*-butyl-2-hydroxyphenyl)phenylphosphine oxide (H_2-(O,O,O))[13] were prepared according to literature procedures. 2-Bromo-4,6-di-*tert*-butylphenol and $PhPCl_2$ were purchased and used as received.

Modified Synthesis of Bis(3,5-di-*tert*-butyl-2-hydroxyphenyl)phenylphosphine (H_2(O,P,O)). The yield of H_2(O,P,O) (40% in the literature)[13] has been improved to 80%, mainly due to the scale-up. A hexane solution of ^{n}BuLi (111 mL of 1.59 M solution, 176 mmol) was added slowly to a diethyl ether (180 mL) solution of 2-bromo-4,6-di-*tert*-butylphenol (25.2 g, 88.3 mmol) at −35 °C. After stirring at room temperature for 6 h, a diethyl ether solution (60 mL) of $PhPCl_2$ (6.0 mL, 44 mmol) was added slowly at −50 °C. The reaction mixture was gradually warmed to 10 °C and stirred overnight. A diethyl ether solution of HCl (90.0 mL of 1.0 M solution, 90.0 mmol) was added to the mixture at 0 °C, and the mixture was stirred at room temperature for 2 h. The solution was centrifuged to remove LiCl. After removal of the solvent under vacuum, the residue was dissolved in acetonitrile (50 mL). The solution was stored at −40 °C to give a white powder of H_2(O,P,O) (18.4 g, 80%). ^{1}H NMR ($CDCl_3$): δ 7.35−7.25 (m, 7H, aromatic H), 6.90 (dd, J = 6.5, 2.1 Hz, 2H, aromatic H), 6.27 (d, J = 8.3 Hz, 2H, OH), 1.42 (s, 18H, ^{t}Bu), 1.14 (s, 18H, ^{t}Bu). $^{31}P\{^1H\}$ NMR ($CDCl_3$): δ −50.5.

Synthesis of (O,P,O)V(SMes)(HNMe$_2$) (2a). A toluene (10 mL) solution of H_2(O,P,O) (342 mg, 0.66 mmol) was slowly added to a toluene (10 mL) solution of **1** (150 mg, 0.66 mmol) at −80 °C. The reaction mixture was gradually warmed to room temperature. The color of the reaction mixture turned from dark green to dark red. After stirring for 2.5 h, a toluene (5 mL) solution of HSMes (201 mg, 1.32 mmol) was added at room temperature. The color of the solution turned to dark yellow. The reaction mixture was stirred for 3.5 h, and the solvent was removed under reduced pressure to give a dark yellow oily material. The residue was washed with pentane (10 mL) to afford an orange powder of **2a** (400 mg, 79%). Single crystals suitable for crystallography were obtained from a THF/pentane solution at −40 °C. UV−vis (THF): λ_{max} = 313 nm (sh, ε 12 000 M^{-1} cm^{-1}), 335 nm (sh, ε 9600 M^{-1} cm^{-1}). ^{1}H NMR (C_6D_6): δ 13.7, 11.5, 6.33, 2.26 (^{t}Bu), 1.23 (^{t}Bu), −3.94, −6.12 (Mes). Cyclic voltammogram (2 mM in THF, potential vs Ag/Ag^+): E_{pc} = 0.55, 0.12, −2.24, −2.65 V, E_{pa} = 0.67, 0.35, 0.18, −1.37 V (irreversible). EPR (microwave power, 1.00 mW; microwave frequency, 9474.082 MHz; modulation width, 0.4 mT; 1 mM in THF): Silent at room temperature. Magnetic susceptibility (B.M.): μ_{eff} = 2.21 (2 K), 2.94 (300 K). Anal. Calcd for $C_{45}H_{63}NO_2PSV$: C, 70.74; H, 8.31; N, 1.83; S, 4.20. Found: C, 71.06; H, 8.18; N, 1.71; S, 4.22.

Synthesis of (O,P,O)V(STip)(HNMe$_2$) (2b). Complex **2b** was prepared from complex **1** (150 mg, 0.66 mmol), H_2(O,P,O) (342 mg, 0.66 mmol), and HSTip (312 mg, 132 mmol) in a similar manner to that used for **2a**. Crystallization from pentane at −40 °C yielded **2b** (213 mg, 39%) as orange crystals. UV−vis (THF): λ_{max} = 326 nm (sh, ε 10 000 M^{-1} cm^{-1}). ^{1}H NMR (C_6D_6): δ 13.7, 6.44, 2.42 (^{t}Bu), 1.24 (^{t}Bu), 1.03 (^{i}Pr of Tip), −1.99, −4.0. Cyclic voltammogram (2 mM in THF, potential vs Ag/Ag^+): E_{pc} = 0.52, 0.06, −0.75, −2.27 V, E_{pa} = 0.71, 0.34, −0.66, −1.36 V (irreversible). EPR (microwave power, 1.00 mW; microwave frequency, 9474.082 MHz; modulation width, 0.4 mT; 1 mM in THF): Silent at room temperature. Magnetic susceptibility (B.M.): μ_{eff} = 2.15 (2 K), 2.51 (300 K). Anal. Calcd for $C_{51}H_{75}NO_2PSV$: C, 72.22; H, 8.91; N, 1.65; S, 3.78. Found: C, 72.70; H, 8.57; N, 1.66; S, 4.05.

Synthesis of (O,O,O)V(SMes)(HNMe$_2$) (3a). Complex **3a** was prepared from complex **1** (150 mg, 0.66 mmol), H_2(O,O,O) (353 mg, 0.66 mmol), and HSMes (201 mg, 132 mmol) in a similar manner to that used for **2a**. Washing the residue with pentane (10 mL) leaves a yellow powder of **3a** (353 mg, 69%). Single crystals suitable for crystallography were obtained from a toluene solution at −40 °C. UV−vis (THF): λ_{max} = 321 nm (ε 12 000 M^{-1} cm^{-1}). ^{1}H NMR (C_6D_6): δ 9.90, 7.97, 6.55, 1.76 (^{t}Bu), 1.23, 1.09 (^{t}Bu), 0.28, −3.34, −7.74 (Mes). Cyclic voltammogram (2 mM in THF, potential vs Ag/Ag^+): E_{pc} = 0.53, 0.12, −2.08, −2.63 V, E_{pa} = 0.70, 0.34, 0.19, −0.57, −1.37 V (irreversible). EPR (microwave power, 1.00 mW; microwave frequency, 9474.082 MHz; modulation width, 0.4 mT; 1 mM in toluene): Silent at room temperature. Magnetic susceptibility (B.M.): μ_{eff} = 1.88 (2 K), 2.55 (300 K). Anal. Calcd for $C_{45}H_{63}NO_3PSV$: C, 69.29; H, 8.14; N, 1.80; S, 4.11. Found: C, 69.79; H, 8.08; N, 1.71; S, 3.74.

Synthesis of (O,O,O)V(STip)(HNMe$_2$) (3b). Complex **3b** was prepared from complex **1** (150 mg, 0.66 mmol), H_2(O,O,O) (353 mg, 0.66 mmol), and HSTip (312 mg, 132 mmol) in a similar manner to that used for **2a**. Washing the residue with pentane (10 mL) leaves a yellow powder of **3b** (228 mg, 40%). Single crystals suitable for crystallography were obtained from a toluene solution at −40 °C. UV−vis (THF): λ_{max} = 321 nm (ε 11 000 M^{-1} cm^{-1}). ^{1}H NMR

dx.doi.org/10.1021/ic4030603 | Inorg. Chem. 2014, 53, 5438−5446

Table 1. Crystal Data for 2a−2b, 3a−3b, 5 and 6

	2a	2b	3a·C_7H_8	3b·$(C_7H_8)_{2.5}$
formula	$C_{45}H_{63}NO_2PSV$	$C_{51}H_{72}NO_2PSV$	$C_{52}H_{71}NO_3PSV$	$C_{68.50}H_{75}NO_3PSV$
formula wt (g mol^{-1})	763.97	845.11	872.11	1074.33
crystal system	orthorhombic	triclinic	monoclinic	monoclinic
space group	$P2_12_12_1$ (No. 19)	$P\bar{1}$ (No. 2)	$P2_1/c$ (No. 14)	$P2_1/n$ (No. 14)
a (Å)	11.9681(13)	12.868(3)	16.251(5)	17.059(3)
b (Å)	13.640(2)	13.695(3)	21.181(6)	17.444(3)
c (Å)	26.614(9)	14.623(3)	16.277(5)	21.669(4)
α (deg)		91.954(3)		
β (deg)		103.666(3)	114.506(4)	94.454(2)
γ (deg)		97.180(3)		
V (Å^3)	4344.4(9)	2478.9(8)	5098(3)	6429(2)
Z	4	2	4	4
D_{calcd} (g/cm^3)	1.168	1.132	1.136	1.110
max 2θ (deg)	55.0	54.9	54.7	54.9
no. of reflections measured	35 477	30 009	40 691	51 636
no. of data used ($I > 2.00\sigma(I)$)	9950	11 253	11 471	14 385
no. of parameters refined	481	527	536	723
$R1$[a]	0.0457	0.0591	0.0493	0.0806
$wR2$[b]	0.1056	0.1691	0.1286	0.2645
GOF[c]	1.071	1.066	1.074	1.056

	5·$(C_4H_8O·C_7H_8)_{0.5}$	6·$(C_5H_{12})_2$
formula	$C_{71}H_{88}Fe_3NO_3PS_5V$	$C_{107}H_{106}Fe_4O_3PS_7V$
formula wt (g mol^{-1})	1413.24	1969.74
crystal system	triclinic	triclinic
space group	$P\bar{1}$ (No. 2)	$P\bar{1}$ (No. 2)
a (Å)	14.50(3)	15.978(3)
b (Å)	16.41(3)	16.111(3)
c (Å)	17.69(3)	22.370(4)
α (deg)	102.80(2)	87.810(6)
β (deg)	93.233(9)	82.923(5)
γ (deg)	114.94(2)	79.975(5)
V (Å^3)	3667(10)	5627(2)
Z	2	2
D_{calcd} (g/cm^3)	1.280	1.163
max 2θ (deg)	51.0	55.0
no. of reflections measured	32 174	69 808
no. of data used ($I > 2.00\sigma(I)$)	13 319	25 680
no. of parameters refined	709	1078
$R1$[a]	0.1629	0.0640
$wR2$[b]	0.4614	0.1992
GOF[c]	1.097	1.011

[a] $I > 2\sigma(I)$, $R1 = \sum||F_o| - |F_c||/\sum|F_o|$. [b] Refined with all data, $wR2 = [\{\sum w(F_o^2 - F_c^2)^2\}/\sum w(F_o^2)^2]^{1/2}$. [c] GOF = $[\{\sum w(F_o^2 - F_c^2)^2\}/(N_0 - N_p)]^{1/2}$, where N_0 and N_p denote the numbers of reflection data and parameters.

(C_6D_6): δ 11.4, 9.81, 8.00, 6.63, 1.71 (^{t}Bu), 1.25, 1.20, 1.09 (^{t}Bu), 0.97, 0.86 (^{i}Pr of Tip), 0.28, −1.44. Cyclic voltammogram (2 mM in THF, potential vs Ag/Ag$^+$): E_{pc} = 0.54, 0.14, −1.53, −2.16 V, E_{pa} = 0.72, 0.35, 0.20, −0.48, −1.37 V (irreversible). EPR (microwave power, 1.00 mW; microwave frequency, 9474.082 MHz; modulation width, 0.4 mT; 1 mM in toluene): Silent at room temperature. Magnetic susceptibility (B.M.): μ_{eff} = 1.98 (2 K), 2.46 (300 K). Anal. Calcd for $C_{51}H_{75}NO_3PSV$: C, 70.88; H, 8.75; N, 1.62; S, 3.71. Found: C, 70.98; H, 8.57; N, 1.68; S, 3.91.

Synthesis of [(O,P,O)VFe$_3$S$_4$(SDmp)(HNMe$_2$)]$_2$ (5). A toluene (10 mL) solution of S_8 (25.2 mg, 0.784 mmol) was added to a toluene (15 mL) solution of **4** (375 mg, 0.588 mmol) at room temperature. After stirring for 2.5 h, a toluene (10 mL) solution of **2a** (150 mg, 0.196 mmol) was added to the solution at room temperature. The reaction mixture was stirred for 3 days, and the solvent was removed under reduced pressure to give a black oily material. The residue was extracted with pentane (10 mL), and the extract was filtered to remove a small amount of insoluble black material. Upon standing at room temperature, black needles of **5** (110 mg, 22%) were obtained. UV−vis (THF): λ_{max} = 326 nm (sh, ε 22 000 M^{-1} cm^{-1}), 442 nm (sh, ε 15 000 M^{-1} cm^{-1}), 559 nm (sh, ε 13 000 M^{-1} cm^{-1}). Cyclic voltammogram (2 mM in THF, potential vs Ag/Ag$^+$): E_{pc} = −1.06 V (irreversible). EPR (microwave power, 1.00 mW; microwave frequency, 9474.082 MHz; modulation width, 0.4 mT; 5 mM in toluene, 8 K): a signal with multiple lines appeared at g = 2.01. Magnetic susceptibility (B.M.): μ_{eff} = 0.89 (2 K), 3.10 (300 K). Anal. Calcd for $C_{120}H_{154}Fe_6N_2O_4P_2S_{10}V_2$: C, 57.46; H, 6.19; N, 1.12; S, 12.79. Found: C, 57.77; H, 5.73; N, 1.33; S, 12.43.

Synthesis of [(μ-O,O,O)VFe$_3$S$_4$(SDmp)(STip)Fe(μ-SDmp)] (6). *Method A.* A toluene (3 mL) solution of **4** (442 mg, 0.694 mmol) was added to a toluene (2 mL) solution of **3b** (150 mg, 0.174 mmol) at room temperature. After stirring for 10 min, a toluene (5 mL) solution of S_8 (22.3 mg, 0.694 mmol) was added at room temperature. The reaction mixture was stirred for 3 days, and the solvent was removed under reduced pressure to give a black oily material. The residue was extracted with pentane (5 mL), and the extract was filtered to remove

dx.doi.org/10.1021/ic4030603 | Inorg. Chem. 2014, 53, 5438−5446

a small amount of insoluble black material. Upon standing at room temperature, black plates of **6** (32 mg, 10%) were obtained. UV−vis (toluene): λ_{max} = 314 nm (ε 24 000 M^{-1} cm^{-1}), 385 nm (sh, ε 7700 M^{-1} cm^{-1}), 420 nm (sh, ε 3600 M^{-1} cm^{-1}). Cyclic voltammogram (2 mM in THF, potential vs Ag/Ag^+): E_{pc} = −0.84 V, E_{pa} = −0.45, −0.73 V (irreversible). EPR (microwave power, 1.00 mW; microwave frequency, 9474.082 MHz; modulation width, 0.4 mT; 5 mM in toluene): Silent in the range of 4−15 K. Magnetic susceptibility (B.M.): μ_{eff} = 2.00 (2 K), 4.80 (300 K). Anal. Calcd for $C_{97}H_{118}Fe_4O_3PS_7V$: C, 62.57; H, 6.39; S, 12.06. Found: C, 62.39; H, 5.97; S, 12.20.

Method B. A toluene (3 mL) solution of **4** (375 mg, 0.589 mmol) was added to a toluene (2 mL) solution of **3a** (150 mg, 0.196 mmol) at room temperature. After stirring for 10 min, a toluene (5 mL) solution of S_8 (25.2 mg, 0.694 mmol) was added at room temperature. The reaction mixture was stirred for 3 days, and the solvent was removed under reduced pressure to give a black oily material. The residue was extracted with pentane (5 mL), and the extract was filtered to remove a small amount of insoluble black material. Upon standing at room temperature, black plates of **6** (29 mg, 8%) were obtained.

X-ray Crystal Structure Determination. Crystallographic data and refinement parameters for **2a−2b**, **3a−3b**, **5**, and **6** are summarized in Table 1. Single crystals were coated with oil (immersion oil, type B: Code 1248, Cargille Laboratories, Inc.) and mounted on loops. Diffraction data were collected at −100 °C under a cold nitrogen stream on a Rigaku RA-Micro7 equipped with a Saturn70 CCD detector, using graphite-monochromated Mo Kα radiation (λ = 0.710690 Å). Six preliminary data frames were measured at 0.5° increments of ω, to assess the crystal quality and preliminary unit cell parameters. The intensity images were also measured at 0.5° intervals of ω. The frame data were integrated using the CrystalClear program package, and the data sets were corrected for absorption using a REQAB program. The calculations were performed with the CrystalStructure program package. All structures were solved by direct methods and refined by full-matrix least-squares. Anisotropic refinement was applied to all non-hydrogen atoms except for disordered atoms (refined isotropically), and all hydrogen atoms were put at calculated positions. Crystals of cluster **5** appear as thin needles, and the quality of their diffraction data was not sufficient. Therefore, some alerts A and B appear in the checking-program of crystallographic data (CIF-check). In **2b**, one *tert*-butyl group is disordered over two positions in a 3:7 ratio. In **5**, a methyl group of toluene (crystal solvent) is disordered over two positions in a 2:3 ratio. In **6**, one *tert*-butyl group is disordered over two positions in a 1:1 ratio.

■ ASSOCIATED CONTENT

Supporting Information

An X-ray crystallographic information file (CIF) for the structures of **2a−6**; molecular structures of **2b** and **3b**; temperature-dependent magnetic susceptibility and cyclic voltammograms of **2a−2b**, **3a−3b**, **5**, and **6**; ^1H NMR spectra of **2a−2b** and **3a−3b**; and EPR spectrum of **5**. This material is available free of charge via the Internet at http://pubs.acs.org.

■ AUTHOR INFORMATION

Corresponding Author

*E-mail: i45100a@nucc.cc.nagoya-u.ac.jp.

Notes

The authors declare no competing financial interest.

■ ACKNOWLEDGMENTS

This research was financially supported by Grant-in-Aids for Scientific Research (Nos. 23000007, 23685015, 25105725, 25109522) from the Ministry of Education, Culture, Sports, Science and Technology, Japan. We are grateful to Prof. Kunio Awaga, Prof. Michio Matsushita, Prof. Hirofumi Yoshikawa, and Dr. Yoshiaki Syuku (Nagoya Univ.) for aiding us with a SQUID-type magnetometer.

■ REFERENCES

(1) (a) Bertini, I.; Sigel, A.; Sigel, H. *Handbook on Metalloproteins*; Marcel Dekker: New York, 2001; Chapter 10. (b) Messerchmidt, A.; Huber, R.; Poulos, T.; Wiehardt, K. *Handbook of Metalloproteins*; John Wiley & Sons: Chichester, U. K., 2001; Vol. *1*, pp 543−552, 560−609.

(2) (a) Vignais, P. M.; Billoud, B. *Chem. Rev.* **2007**, *107*, 4206−4272. (b) Fontecilla-Camps, J. C.; Volbeda, A.; Cavazza, C.; Nicolet, Y. *Chem. Rev.* **2007**, *107*, 4273−4303. (c) De Lacey, A. L.; Fernández, V. M.; Rousset, M.; Cammack, R. *Chem. Rev.* **2007**, *107*, 4304−4330. (d) Tard, C.; Pickett, C. J. *Chem. Rev.* **2009**, *109*, 2245−2274.

(3) (a) Ragsdale, S. W.; Kumar, M. *Chem. Rev.* **1996**, *96*, 2515−2539. (b) Ragsdale, S. W. *Crit. Rev. Biochem. Mol. Biol.* **2004**, *39*, 165−195. (c) Hegg, E. L. *Acc. Chem. Res.* **2004**, *37*, 775−783. (d) Messerchmidt, A. *Handbook of Metalloproteins*; John Wiley & Sons: Chichester, U. K., 2011; Vol. *4*, pp 387−396, 397−412.

(4) (a) Howard, J. B.; Rees, D. C. *Chem. Rev.* **1996**, *96*, 2965−2982. (b) Burgess, B. K.; Lowe, D. J. *Chem. Rev.* **1996**, *96*, 2983−3012. (c) Einsle, O.; Tezcan, F. A.; Andrade, S. L. A.; Schmid, B.; Yoshida, M.; Howard, J. B.; Rees, D. C. *Science* **2002**, *297*, 1696−1700. (d) Spatzal, T.; Aksoyoglu, M.; Zhang, L.; Andrade, S. L. A.; Schleicher, E.; Weber, S.; Rees, D. C.; Einsle, O. *Science* **2011**, *334*, 940. (e) Lancaster, K. M.; Roemelt, M.; Ettenhuber, P.; Hu, Y.; Ribbe, M. W.; Neese, F.; Bergmann, U.; DeBeer, S. *Science* **2011**, *334*, 974−977.

(5) (a) Eady, R. R. *Chem. Rev.* **1996**, *96*, 3013−3030. (b) Eady, R. R. *Coord. Chem. Rev.* **2003**, *237*, 23−30. (c) Fay, A. W.; Blank, M. A.; Lee, C. C.; Hu, Y.; Hodgson, K. O.; Hedman, B.; Ribbe, M. W. *J. Am. Chem. Soc.* **2010**, *132*, 12612−12618.

(6) (a) Lindahl, P. A. *Biochemistry* **2002**, *41*, 2097−2105. (b) Jeoung, J.-H.; Dobbek, H. *Science* **2007**, *318*, 1461−1464.

(7) (a) Osterloh, F.; Sanakis, Y.; Staples, R. J.; Münck, E.; Holm, R. H. *Angew. Chem., Int. Ed.* **1999**, *38*, 2066−2070. (b) Osterloh, F.; Achim, C.; Holm, R. H. *Inorg. Chem.* **2001**, *40*, 224−232. (c) Zhang, Y.; Zuo, J.-L.; Zhou, H.-C.; Holm, R. H. *J. Am. Chem. Soc.* **2002**, *124*, 14292−14293. (d) Zhang, Y.; Holm, R. H. *J. Am. Chem. Soc.* **2003**, *125*, 3910−3920. (e) Zhang, Y.; Holm, R. H. *Inorg. Chem.* **2004**, *43*, 674−682. (f) Berlinguette, C. P.; Miyaji, T.; Zhang, Y.; Holm, R. H. *Inorg. Chem.* **2006**, *45*, 1997−2007. (g) Berlinguette, C. P.; Holm, R. H. *J. Am. Chem. Soc.* **2006**, *128*, 11993−12000. (h) Hlavinka, M. L.; Miyaji, T.; Staples, R. J.; Holm, R. H. *Inorg. Chem.* **2007**, *46*, 9192−9200.

(8) (a) Ciurli, S.; Yu, S.-B.; Holm, R. H.; Srivastava, K. K. P.; Münck, E. *J. Chem. Soc.* **1990**, *112*, 8169−8171. (b) Ciurli, S.; Ross, P. K.; Scott, M. J.; Yu, S.-B.; Holm, R. H. *J. Am. Chem. Soc.* **1992**, *114*, 5415−5423. (c) Zhou, J.; Scott, M. J.; Hu, Z.; Peng, G.; Münck, E.; Holm, R. H. *J. Am. Chem. Soc.* **1992**, *114*, 10843−10854. (d) Panda, R.; Zhang, Y.; McLauchlan, C. C.; Rao, P. V.; Tiago de Oliveira, F. A.; Münck, E.; Holm, R. H. *J. Am. Chem. Soc.* **2004**, *126*, 6448−6459. (e) Panda, R.; Berlinguette, C. P.; Zhang, Y.; Holm, R. H. *J. Am. Chem. Soc.* **2005**, *127*, 11092−11101. (f) Sun, J.; Tessier, C.; Holm, R. H. *Inorg. Chem.* **2007**, *46*, 2691−2699.

(9) (a) Tyson, M. A.; Coucouvanis, D. *Inorg. Chem.* **1997**, *36*, 3808−3809. (b) Han, J.; Beck, K.; Ockwing, N.; Coucouvanis, D. *J. Am. Chem. Soc.* **1999**, *121*, 10448−10449. (c) Coucouvanis, D.; Han, J.; Moon, N. *J. Am. Chem. Soc.* **2002**, *124*, 216−224.

(10) (a) Ohki, Y.; Sunada, Y.; Honda, M.; Katada, M.; Tatsumi, K. *J. Am. Chem. Soc.* **2003**, *125*, 4052−4053. (b) Ohki, Y.; Ikagawa, Y.; Tatsumi, K. *J. Am. Chem. Soc.* **2007**, *129*, 10457−10465. (c) Ohki, Y.; Imada, M.; Murata, A.; Sunada, Y.; Ohta, S.; Honda, M.; Sasamori, T.; Tokitoh, N.; Katada, M.; Tatsumi, K. *J. Am. Chem. Soc.* **2009**, *131*, 13168−13178. (d) Ohki, Y.; Murata, A.; Imada, M.; Tatsumi, K. *Inorg. Chem.* **2009**, *48*, 4271−4273. (e) Hashimoto, T.; Ohki, Y.; Tatsumi, K. *Inorg. Chem.* **2010**, *49*, 6102−6109. (f) Ohta, S.; Ohki, Y.; Hashimoto, T.; Cramer, R. E.; Tatsumi, K. *Inorg. Chem.* **2012**, *51*, 11217−11219. (g) Ohki, Y.; Tanifuji, K.; Yamada, N.; Cramer, R. E.; Tatsumi, K. *Chem.—Asian J.* **2012**, *7*, 2222−2224.

(11) (a) Ohki, Y.; Sunada, Y.; Tatsumi, K. *Chem. Lett.* **2005**, *34*, 172−173. (b) Ohki, Y.; Tanifuji, K.; Yamada, N.; Imada, M.; Tajima, T.; Tatsumi, K. *Proc. Natl. Acad. Sci. U.S.A.* **2011**, *108*, 12635−12640.
(12) (a) Haaland, A.; Rypdal, K.; Volden, H. V.; Andersen, R. A. *J. Chem. Soc., Dalton Trans.* **1992**, 891−895. (b) Dubberley, S. R.; Tyrrell, B. R.; Mountford, P. *Acta Crystallogr.* **2001**, *C57*, 902−904.
(13) Siefert, R.; Weyhermüller, T.; Chaudhuri, P. *J. Chem. Soc., Dalton Trans.* **2000**, 4656−4663.
(14) (a) Paine, T. K.; Weyhermüller, T.; Slep, L. D.; Neese, F.; Bill, E.; Bothe, E.; Wieghardt, K.; Chaudhuri, P. *Inorg. Chem.* **2004**, *43*, 7324−7338. (b) Liang, L. C.; Chang, Y. N.; Lee, H. M. *Inorg. Chem.* **2007**, *46*, 2666−2673. (c) Carmichael, C. D.; Fryzuk, M. D. *Can. J. Chem.* **2010**, *88*, 667−675.
(15) Krzystek, J.; Ozarowski, A.; Telser, J. *Coord. Chem. Rev.* **2006**, *250*, 2308−2324.
(16) Randall, C. R.; Armstrong, W. H. *Chem. Commun.* **1988**, 986−987.
(17) (a) Magill, C. P.; Floriani, C.; Chiesi-Villa, A.; Rizzoli, C. *Inorg. Chem.* **1993**, *32*, 2729−2735. (b) Witte, P. T.; Meetsma, A.; Hessen, B. *Organometallics* **1999**, *18*, 2944−2946. (c) Lee, I. S.; Long, J. R. *Dalton Trans.* **2004**, 3434−3436.
(18) (a) Hauser, C.; Bill, E.; Holm, R. H. *Inorg. Chem.* **2002**, *41*, 1615−1624. (b) Zuo, J.-L.; Zhou, H.-C.; Holm, R. H. *Inorg. Chem.* **2003**, *42*, 4624−4631. (c) Scott, T. A.; Holm, R. H. *Inorg. Chem.* **2008**, *46*, 3426−3432.
(19) The EPR spectra at higher than 20 K are not discussed for clusters in this study because fast relaxation is known for iron−sulfur clusters. See for examples: (a) Guigliarelli, B.; Bertrand, P. *Adv. Inorg. Chem.* **1997**, *47*, 421−497. (b) Rao, P. V.; Holm, R. H. *Chem. Rev.* **2004**, *104*, 527−559.
(20) Werth, M. T.; Kurtz, D. M., Jr.; Howes, B. D.; Huynh, B. H. *Inorg. Chem.* **1989**, *28*, 1357−1361.
(21) (a) Ellison, J. J.; Ruhlandt-Senge, K.; Power, P. P. *Angew. Chem., Int. Ed. Engl.* **1994**, *33*, 1178−1180. (b) Ohta, S.; Ohki, Y.; Ikagawa, Y.; Suizu, R.; Tatsumi, K. *J. Organomet. Chem.* **2007**, *692*, 4792−4799.
(22) (a) Do, Y.; Simhon, E. D.; Holm, R. H. *Inorg. Chem.* **1985**, *24*, 4635−4642. (b) Kovacs, J. A.; Holm, R. H. *J. Am. Chem. Soc.* **1986**, *108*, 340−341. (c) Kovacs, J. A.; Holm, R. H. *Inorg. Chem.* **1987**, *26*, 711−718. (d) Carney, M. J.; Kovacs, J. A.; Zhang, Y.-P.; Papaefthymiou, G. C.; Spartalian, K.; Frankel, R. B.; Holm, R. H. *Inorg. Chem.* **1987**, *26*, 719−724. (e) Ciurli, S.; Holm, R. H. *Inorg. Chem.* **1989**, *28*, 1685−1690. (f) Cen, W.; Lee, S. C.; Li, J.; MacDonnell, F. M.; Holm, R. H. *J. Am. Chem. Soc.* **1993**, *115*, 9515−9523. (g) Malinak, S. M.; Demadis, K. D.; Coucouvanis, D. *J. Am. Chem. Soc.* **1995**, *117*, 3126−3133. (h) Huang, J.; Mukerjee, S.; Segal, B. M.; Akashi, H.; Zhou, J.; Holm, R. H. *J. Am. Chem. Soc.* **1997**, *119*, 8662−8674. (i) Deng, Y.; Liu, Q.; Chen, C.; Wang, Y.; Cai, Y.; Wu, D.; Kang, B.; Liao, D.; Cui, J. *Polyhedron* **1997**, *16*, 4121−4128. (j) Zhang, Y.; Liu, Q.; Deng, Y.; Zhu, H.; Chen, C.; Liao, D.; Cui, J. *Polyhedron* **1999**, *18*, 3153−3163. (k) Fomitchev, D. V.; McLauchlan, C. C.; Holm, R. H. *Inorg. Chem.* **2002**, *41*, 958−966.
(23) Pangborn, A. B.; Giardello, M. A.; Grubbs, R. H.; Rosen, R. K.; Timmers, F. J. *Organometallics* **1996**, *15*, 1518−1520.
(24) Chisholm, M. H.; Corning, J. F.; Huffman, J. C. *Inorg. Chem.* **1984**, *23*, 754−757.
(25) Blower, P. J.; Dilworth, J. R.; Hutchinson, J. P.; Zubieta, J. A. *J. Chem. Soc., Dalton Trans.* **1985**, 1533−1541.